Aeolian Research 31 (2018) 3–17

Contents lists available at ScienceDirect

Aeolian Research

journal homepage: www.elsevier.com/locate/aeolia

Coastal dune dynamics in response to excavated foredune notches

B.G. Ruessink [a,*], S.M. Arens [b], M. Kuipers [c], J.J.A. Donker [a]

[a] Department of Physical Geography, Faculty of Geosciences, Utrecht University, P.O. Box 80.115, 3508 TC Utrecht, The Netherlands
[b] Bureau for Beach and Dune Research, Soest, The Netherlands
[c] PWN Drinking Water Company, Velserbroek, The Netherlands

ARTICLE INFO

Article history:
Received 23 February 2017
Revised 20 June 2017
Accepted 4 July 2017
Available online 17 July 2017

Keywords:
Dune restoration
Foredune notches
Airborne Lidar
Unmanned Aerial Vehicle
Coastal dunes
Topographic surveys

ABSTRACT

Dune management along developed coasts has traditionally focussed on the suppression of the geomorphic dynamics of the foredune to improve its role in sea defence. Because a stabilized foredune acts as an almost total barrier to aeolian transport from the beach, the habitat diversity in the more landward dunes has degraded. With the overarching objective to mitigate this undesirable loss in biodiversity, dune management projects nowadays increasingly intend to restore aeolian dynamics by reconnecting the beach-dune system with notches excavated through the foredune. Here, we use repeat topographic survey data to examine the geomorphic response of a coastal dune system in the Dutch National Park Zuid-Kennemerland to five notches excavated in 2012–2013 within an 850-m stretch of the 20-m high established foredune. The notches were dug in a V-shape (viewed onshore), with a width between approximately 50 and 100 m at the top, a (cross-dune) length between 100 and 200 m, and excavation depths between 9 and 12.5 m. The 1×1 m digital terrain models, acquired with airborne Lidar and UAV photogrammetry, illustrate that during the 3-year survey period the notches developed into a U-shape because of wall deflation, and that up to 8-m thick and 150-m long depositional lobes formed landward of the notches. Sand budget computations showed that the sand volume of the entire study area increased by about 22,750 m^3/year, which, given the 850-m width of the study area, corresponds to an aeolian input from the beach of approximately 26.5 m^3/m/year. Between 2006 and 2012 all wind-blown beach sand deposited on the seaward side of the foredune; since 2013, the notches have caused 75% of the sand to be deposited landward of the foredune. This highlights that the notches are highly effective conduits for aeolian transport into the back dunes. Future monitoring is required to determine for how long the notches will stimulate aeolian dynamics and if (and when) vegetation eventually starts to regrow and enforces the degeneration of the notches.

1. Introduction

Coastal dunes are natural, intrinsically important landform units in the coastal system and provide a wide range of benefits to humankind (e.g., Everard et al., 2010). For example, they act as a vital natural safety barrier against marine flooding, are valuable natural environments, serve for the production of drinking water, and offer recreational opportunities. The safety function has dominated dune management along low-lying developed shores for decades (Arens and Wiersma, 1994; Jackson and Nordstrom, 2011). Planting vegetation is a common practice to increase height and volume of the foredune (e.g., Van der Putten and Peters, 1995; Nordstrom and Arens, 1998). The resulting dune stabilization is considered crucial to safeguard coastal dune systems and low-elevation coastal areas against expected increases in erosion because of global-change induced rising sea levels and potential changes in storm characteristics (e.g., Sigrin et al., 2014; Feagin et al., 2015). While foredune stabilization substantially reduces the risk of marine flooding of the hinterland, it also degrades aesthetic and natural values and markedly reduces species diversity in the back dunes (Martínez et al., 2013). The dense vegetation cover on a managed foredune acts as a barrier to the aeolian throughput of sand from the beach into the back dunes (e.g., Petersen et al., 2011), where spatio-temporal dynamics have thus become limited and ecological succession is no longer locally reset by sand burial. Consequently, many back dune systems suffer from the encroachment of tall grasses and shrubs (e.g., Veer and Kooijman, 1997; Van Til et al., 2002; Hilton, 2006; Lammerts et al., 2009; Pye et al.,

* Corresponding author.
E-mail addresses: b.g.ruessink@uu.nl (B.G. Ruessink), arens@duinonderzoek.nl (S.M. Arens), marieke.kuipers@pwn.nl (M. Kuipers), j.j.a.donker@uu.nl (J.J.A. Donker).
URL: http://www.uu.nl/staff/bgruessink (B.G. Ruessink).

http://dx.doi.org/10.1016/j.aeolia.2017.07.002
1875-9637/

2014) and reduced biodiversity. This is further exacerbated by increased atmospheric nitrogen deposition, changed land use within the dune system, reduced disturbance by rabbit populations, and stabilization of local bare-sand areas (e.g., Nordstrom and Lotstein, 1989; Provoost et al., 2011). The encroachment by tall grasses and shrubs further reduces the amount of sunlight reaching the surface and potentially causes (internal) soil acidification, which is strongly disadvantageous to the endemic dune flora (Kooijman, 2004). The blocked aeolian input of sand also prevents the back dunes to grow vertically with sea-level rise, which may endanger future coastal safety (Arens et al., 2013).

Since the late 1980s a wide variety of measures to maintain or, preferably, improve coastal-dune biodiversity have been attempted (see Lithgow et al., 2013, for a review). In the Netherlands, which holds major responsibility for the preservation of coastal-dune biodiversity within Europe because of its spatially extensive dune fields, initial measures aimed at resetting ecological succession through the removal of vegetation and topsoil in dune slacks (e.g., Jungerius et al., 1995). While some measures were, at least in part, successful (Grootjans et al., 2002), awareness grew that restored ecosystems could be self-maintaining (i.e., demanding no or minimal further management) when aeolian dynamics are re-established (e.g., Arens and Geelen, 2001). This started with the restoration of individual blowouts, but its impact on landscape-scale aeolian dynamics and hence ecology proved to be minimal (Van Boxel et al., 1997). Landscape-scale measures, such as the reactivation of parabolic dunes by vegetation removal, increased aeolian dynamics dramatically during the first few years (Arens et al., 2004), resulting in the desired burial of tall grasses and shrubs downwind and thus in the development of more diverse habitat types. However, these interventions have not been self-maintaining (Arens and Geelen, 2006; Arens et al., 2013). Most sites began to stabilize because of vegetation regrowth from remaining rhizomes and the seed bank, and the reduction in aeolian erosion through the formation of a lag of dead root material. In line with an international management shift toward more foredune dynamics (e.g., Jackson et al., 2013; Walker et al., 2013; Pye et al., 2014; Konlechner et al., 2015; Darke et al., 2016), the present Dutch dune management strategy seeks to connect landscape-scale restoration efforts of back dunes with the beach-foredune system through the excavation of foredune notches (e.g., Arens et al., 2012, 2013; Kuipers, 2014). In this way, one of the major causes of ecosystem degradation in the back dunes is removed, potentially providing a self-maintaining ecosystem with minimal need for further management (Elliott et al., 2007). It is expected that notches will act as a conduit for the transport of wind-blown beach sand to the back dunes. Potentially, the notches could develop into more natural, self-maintaining foredune gaps, ensuring a sustained influx of calcareous beach sand. Furthermore, the notches may produce harsher living conditions in the back dunes (e.g., higher wind speeds and salt spray), increasing aeolian dynamics and impeding vegetation regrowth on reactivated areas.

An increasing number of coastal restoration projects involve excavating foredune notches, however, experience with their performance is limited. Meerkerk et al. (2007) examined the sand transport dynamics through a single 60-m wide gap in the foredune near Schoorl, the Netherlands, that was excavated to a depth that would allow marine flooding during severe storms. However, wind-blown beach sand quickly filled the gap. Aeolian dynamics was found to be at a maximum 3 years after the excavation, with calcareous beach sand blown up to 350 m inland. However, aeolian processes then diminished as vegetation started to grow in the (almost) closed gap. Schupp et al. (2013) reported on 14 30-m wide notches cut through a low, constructed foredune at Assateague Island, Maryland, USA, to stimulate overwash processes. Although some of the sediment subsequently deposited on the island's interior may have been aeolian in nature, this was not further investigated. Pye and Blott (2016) examined the evolution of 27 notches at 3 sites in Wales, which had typical (alongshore) widths of 20–30 m, lengths between 22 and 185 m, and maximum excavation depths between 0.2 and 8 m. The occasional shallow excavation depths were imposed to prevent marine flooding during severe storms. Following their excavation, all notches were seen to deliver sand inland, deposited as lobes at the landward notch ends. The degree of aeolian dynamics depended on the beach sediment budget. In general, the largest dynamics were observed where notches fronted rather wide, high beaches (i.e., positive beach sediment budget). Notches that forced the wind to accelerate because of, for example, a convex notch floor or notch narrowing in the landward direction, were more effective in stimulating landward aeolian transport (Pye and Blott, 2016). Finally, Riksen et al. (2016) measured an influx of sand through three notches on the barrier island of Ameland, the Netherlands, to some 50 m from the foredune crest. They ascribed this rather limited distance to the small width (about 20 m) of the notches and their large alongshore separation.

The aim of this paper is to quantify and interpret the geomorphic dynamics of a (fore)dune system in response to the excavation of five notches in the approximately 20-m high foredune of National Park Zuid-Kennemerland, the Netherlands. In comparison to the notches mentioned above, the present notches are relatively closely spaced (the study site measures 850 m in the alongshore direction), wide (50–100 m at the top), and deep (maximum excavation depths of 9–12.5 m). After a brief description of the study site and the restoration project (Section 2), the airborne-Lidar and UAV-photogrammetry methodology adopted to collect topographic surveys during the 3-year observational period is outlined, including an assessment of survey accuracy (Section 3). Two-dimensional (2D) profiles and three-dimensional (3D) digital terrain models are used to quantify geomorphic changes and sand budget responses on the seaward slope of the foredune, in the notches, and in the dunes further landward (Section 4). In Section 5 we discuss the notches' potential future evolution. The main conclusions of our work are stated in Section 6.

2. Study area

The study area is an approximately 850-m stretch of frontal coastal dunes located in the National Park Zuid-Kennemerland (NPZK) near Bloemendaal, the Netherlands (between regional beach poles with km-indication 59,25 and 60,25). A continuous, approximately 20-m high established foredune existed along the entire study area prior to notch excavation (Fig. 1a). The foredune was almost fully covered by European marram grass (*Ammophila arenaria*) and resembled a linear sand dyke because of decades of management to minimize sand loss (e.g., Klijn, 1981; De Ruig and Hillen, 1997). Management measures, carried out by the Rijnland District Water Control Board until 1984 (Arens, 1999), consisted of the adjustment of the seaward foredune slope with ground-moving equipment, the planting of marram grass and the placing of sand fences (Bochev-van der Burgh et al., 2011). The cessation of management measures in 1984 has given the foredune a slightly more natural look (e.g., the formation of embryo dunes) compared with the coast a few kilometers to the south, where management persisted until 1990 (Arens, 1999). The sediment budget at the site has been moderately positive for the last decades (Luijendijk et al., 2011). To provide insight into foredune dynamics in the years leading up to notch excavation, we examined annual airbone Lidar surveys (see Section 3.1 below for details) available on a 1×1 m grid since 2006. During the period 2006–2012 surface elevation z (with respect to Mean Sea Level, MSL) changed most

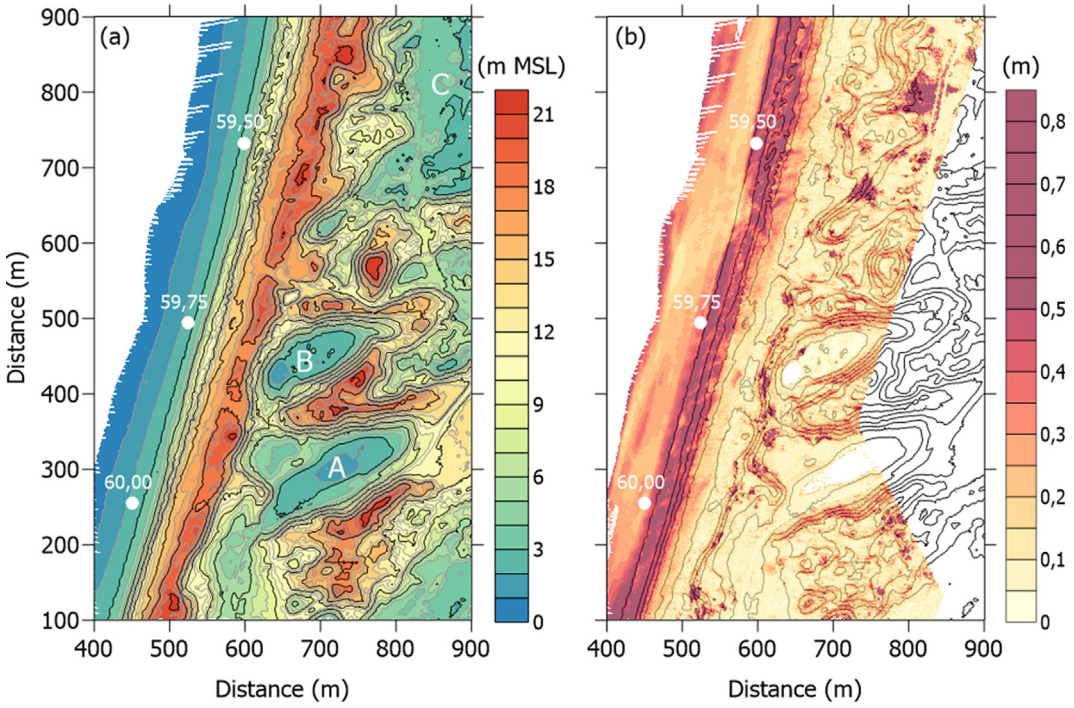

Fig. 1. (a) Elevation z with respect to Mean Sea Level (MSL) in the study site prior to notch excavation, here based on the airborne lidar survey of February 2006 and (b) spatial distribution of the root-mean-square elevation difference Δz_{rms} based on annual airborne lidar surveys from 2006 up to and including 2012 (see Section 3.1). In (a) the major black contours start at 3 m above MSL and have a 3-m interval. The minor grey contours have a 1-m interval. A, B and C are the dune slacks called Peperedel, Kattendel and Houtglop, respectively. The white dots represent beach poles with their km-location, which are distance markers that can be found along the entire Dutch coast. To compute Δz_{rms} the 7 annual lidar data sets were differenced into 6 annual difference models (i.e., 2007–2006, 2008–2007, etc.). ΔZ_{rms} is the root-mean-square value of the six elevation differences in each grid cell; ΔZ_{rms} values are only shown in (b) if they could be based on all 6 difference models. The black contours in (b) are the same as in (a).

between the 2 and 15-m contours seaward of the foredune crest, with only minor variability further landward (Fig. 1b). The foredune was predominantly progradational (Fig. 2) with an annual deposition of sand between the 2-m contour and the dune crest that increased from approximately 15–20 m^3/m in the southern to 25–35 m^3/m in the northern part of the study area. The alongshore average deposition was $\approx 27\ m^3/m$/year. Landward of the foredune two southwest-northeast oriented parabolic dunes can be seen (Fig. 1a); their dune slacks are locally known as Peperedel (location A in Fig. 1a) and Kattendel (location B). Further north, location C marks part of a dune slack belonging to a substantially larger parabolic dune (Houtglop) that is to the northeast of the study area. The width of the beach between the low-tide line (−0.75 m MSL) and the 2-m contour (i.e., the wet and dry beach combined) is of the order of 100 m. The wet beach often contains a single sandbar.

The wind climate at the study site was assessed using hourly wind speeds and direction measured for the period 2001–2015 at station 225 (IJmuiden) of the Royal Netherlands Meteorological

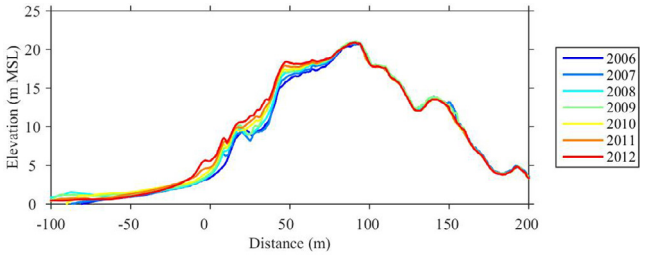

Fig. 2. Elevation with respect to Mean Sea Level (MSL) versus cross-shore distance between 2006 and 2012 in profile 59,50 (see Fig. 1). The beach is on the left.

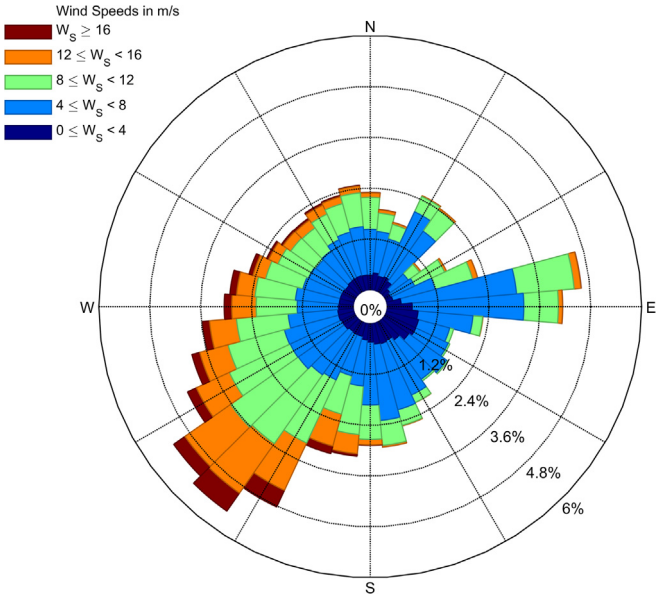

Fig. 3. Wind rose from station 225 (IJmuiden) of the Royal Netherlands Meteorological Institute KNMI (2001–2015). This station is located some 4 km north of the study area at the landward end of the southern IJmuiden harbour mole, close to the transition from the beach to the foredune. The relatively large fraction of easterly winds is potentially a local phenomenon, reflecting the effect of the east-west oriented Noordzeekanaal (located landward of the wind station) on the regional wind field. Wind roses based on data collected on the North Sea, or elsewhere along the coast, do not show this peak in easterly winds.

Institute KNMI. This station is located some 4 km north of the study site at the landward end of the southern IJmuiden harbour mole, close to the transition from the beach to the foredune. As can be seen in Fig. 3, the strongest and most frequent winds are from the southwest. Because the shore-normal direction is approximately 287°N, these winds are thus strongly onshore shore-oblique. Winds with speeds in excess of 12 m/s can also come from westerly to northwesterly directions, but these are substantially less frequent (Fig. 3). These northwesterly winds are, however, often associated with a surge that can exceed 1 m, which, together with high ($>$ 5 m) waves, can lead to the (partial) destruction of the embryo dunes and to foredune scarping, similar to that observed elsewhere along the Dutch coast (e.g., De Winter et al., 2015). The median grain size of the foredune is 200–250 μm (e.g., Koshiek, 1984).

In 2012 and 2013 various measures were taken in NPZK to restore dune mobility (Figs. 4 and 5a–b) and, in this way, to extend the area of the Nature 2000 habitat White Dunes (H2120; mobile coastal dunes) as well as to improve conditions for habitat Grey Dunes (H2130; fixed coastal dunes with herbaceous vegetation). The measures were all part of the Noordwest Natuurkern project (Kuipers, 2014; Kuipers et al., 2016), a joint effort of PWN (the regional drinking water company, also responsible for nature management in the dunes), Natuurmonumenten (the largest Dutch private organisation for nature conservation) and the Rijnland District Water Control Board. The measures comprised two parts, the reactivation of existing parabolic dunes and the excavation of foredune notches. Three in-land parabolic dunes (Cremermeer, Wieringen Noord and Wieringen Zuid) were reactivated by vegetation and soil removal between January and March 2012, with similar measures at other parabolic dunes, including those embracing Peperedel, Kattendel (Fig. 4, labeled U1 and U2, respectively) and Houtglop between October 2012 and March 2013. During this latter period five notches were additionally excavated in the foredune between (beach) km-poles 59.25 and 60.25 (Fig. 4, labeled N1 to N5 from south to north). The notches were dug through the entire foredune, starting at approximately 6 m above MSL on the seaward side of the foredune and ending at about 9 m above MSL on the landward side. The notch floor had an approximately linear slope between these two points, resulting in a (cross-dune) length of about 100 m for N1–N3, 130 m for N4 and 200 m for N5. The notches were dug in a V-shape (viewed onshore), with a width between approximately 50 m (N2) to 100 m (N1) at the top. The maximum excavation depth varied between approximately 9 m in N3 to 12.5 m in N5. In total, some 170,000 m^3 of sand was removed from the foredune, all of which was reused elsewhere in NPZK (but outside our study area; see Kuipers (2014), for details). The total surface area of the notches amounted to about 42,000 m^2. While N1–N3 are oriented approximately shore-normally, the two northern notches (N4 and N5) are oriented like the inland parabolic dunes (southwest-northeast). From 2013 onward some minor interventions had to be performed in the notches, as detailed in Arens et al. (2016). Marram grass was removed manually from the seaward side of the notches in 2013 and 2014. In addition, gravel paving on the sand surface was also removed. This rubble is composed of generally small (a few cm max) concrete blocks that originate from the many World War II Atlantic Wall bunkers in the area. Occasionally, larger slabs of concrete that came to the surface because of erosion were also removed. Finally, it is important to note that N1 serves as a beach entry and ends near a bicycle track and a large wooden structure where bikes can be parked. This structure soon became (partly) buried by sand blown through N1. In 2013 and 2014 about 2200–2500 m^3 of sand was returned to the seaward side of N1 with ground-moving equipment. In 2015 the wooden structure was repositioned southward, but sand accumulating on the bicycle track was still removed (about 1500 and 900 m^3 in 2015 and 2016, respectively). All other notches are closed to the public.

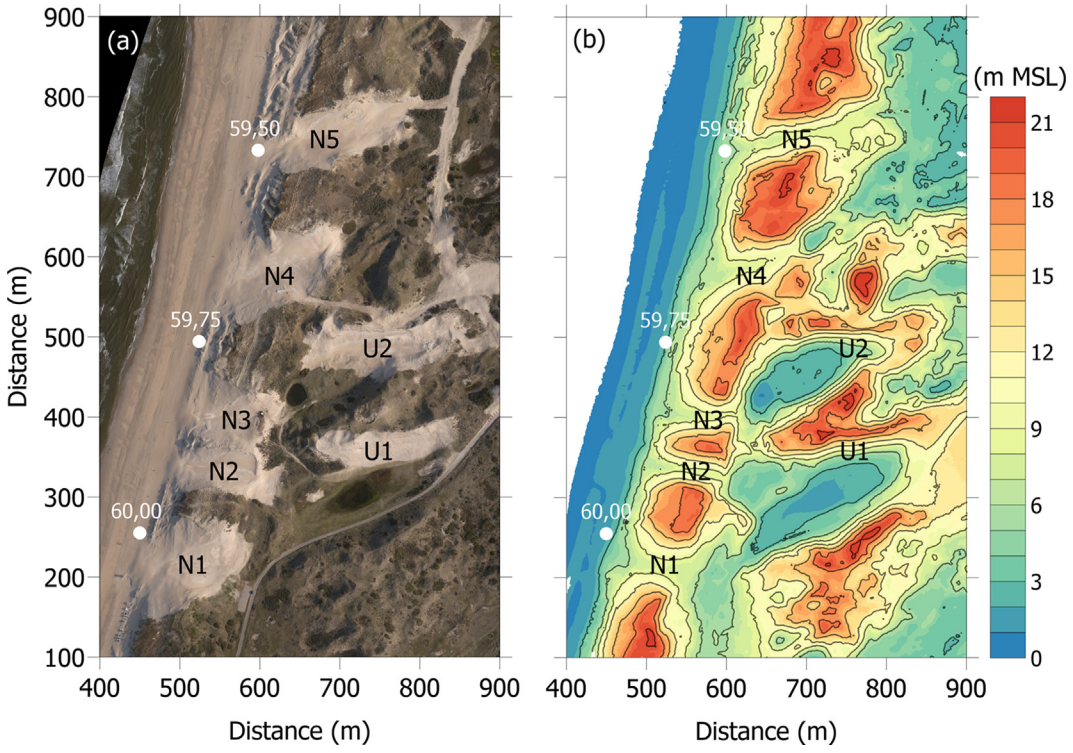

Fig. 4. Overview of (fore)dune restoration measures as part of the Noordwest Natuurkern project with (a) orthophoto and (b) elevation z with respect to Mean Sea Level (MSL). The five notches through the foredune are labeled N1 to N5. The two de-vegetated steep slopes of the Peperdel and Kattendel parabolic dunes are labeled U1 and U2. The aerial photograph is the merged orthophoto based of the May13 UAV survey, see Table 1, and the elevation map is the Digital Terrain Model estimated from this survey, see Section 3.2. The thin black lines in (b) are bed-elevation contours, starting at 3 m MSL and with a 3-m interval.

Fig. 5. Photographs of (a) the five foredune notches (July 21, 2013), (b) notch 2 (July 21, 2013), (c–d) deposition lobes landward of N2 (July 21, 2013) and N5 (April 20, 2016), respectively, and (e) composite notch wall in N2 (April 20, 2016).

3. Methodology

3.1. Airborne Lidar

Topographic data of the entire Dutch coastal zone have been collected annually with airborne LIDAR (ALS) since 1996 (Bochev-van der Burgh et al., 2011). The surveys are commissioned by the Dutch governmental organization Rijkswaterstaat and have been carried out by various commercial contractors using different Lidar operating systems. The data are publicly available as DEMs with a 5 × 5 m and, since 2013, a 2 × 2 m resolution, both of which are too coarse for an accurate representation of the dune topography (e.g., Woolard and Colby, 2002; Hesp et al., 2016). Therefore, we requested the three-dimensional (3D) point clouds of ground-surface values for our study area, which were available since 2006. We processed the available data into 1 × 1-m DEMs with a local west-east x coordinate from 400 to 900 m, and a local south-north y coordinate from 100 to 900 m. To transform these local coordinates to the Dutch RD system, 98,000 m has to be added to x, and 493,000 m to y. The elevation z was computed as the average z of all points within a 1-m radius around any grid point. Data point density varied spatially and between years, with, on average, 3.8 points/m^2. Small holes with missing z were replaced with z interpolated smoothly from the values neighboring the holes (D'Errico, 2004). The aforementioned pre-notch foredune evolution was based on the 2006–2012 1 × 1-m DEMs. We will use the 2012–2016 1 × 1-m DEMs in the remainder of this paper to examine the dynamics of the study area since notch excavation, with the 2012 DEM serving as the pre-notch topography. Table 1 lists all flight dates. We will henceforth adopt a MMMYY coding (MMM = month, YY = year; for example, Feb12) to refer to individual surveys. The Jan13 survey was flown during notch excavation, with work being finished in notches 4 and 5 only. Additional airborne Lidar surveys of the study site were performed in January 2014 and March 2015. The Jan14 survey was collected in the framework of the third digital elevation model of the Netherlands (the so-called third Actueel Hoogtebestand Nederland, or AHN3), while the Mar15 survey was commissioned by PWN as part of the Noordwest Natuurkern project.

The elevation accuracy demanded by Rijkswaterstaat is specified as a maximum bias $b_{z,\max}$ of 0.05 m and a maximum standard deviation $s_{z,\max}$ of 0.1 m. This implies that 95% of the points should have an elevation error within $b_{z,\max} \pm 2s_{z,\max}$ m. Data quality documents illustrate that this accuracy, assessed with data collected over reference areas, was always met. It is possible that the elevation accuracy is less in vegetated dune regions. To examine this, we computed 4 annual difference Δz models (i.e., 2013–2012, 2014–2013, 2015–2014, 2016–2015) for the region bound by $x = [650 - 900]$ m and $y = [100 - 200]$ m, as this region remained mostly vegetated after notch excavation and presumably experienced negligible elevation change. The mean Δz varied between −0.047 and 0.058 m, and the standard deviation in Δz between 0.08 and 0.10 m. This suggests that elevation accuracy in vegetated regions is also within or close to the desired specification. Computations for the same region illustrate that the accuracy of the two additional Lidar surveys was comparable to that of the standard annual surveys.

3.2. UAV photogrammetry

3.2.1. Approach

Additional topographic data were obtained between May 2013 and April 2016 (Table 1) from highly overlapping images collected with an Unmanned Aerial Vehicle (UAV), a technique that is

Table 1
Summary of collected data.

Date	Source	Point density [1] (pt m^{-2})	Number of images [2]	Number of GCPs [2]	Remark[3]
20 Feb. 2012	ALS	3.5			CL; pre-notch survey
14 Jan. 2013	ALS	3.4			CL; work in N4 and N5 completed
1 May 2013	UAV	57.5	unk	9	work in all notches completed
30 Jan. 2014	ALS	22.2			AHN3
8 Mar. 2014	ALS	3.7			CL
10 Apr. 2014	UAV	97.4	955	28	year 1
28 Oct. 2014	UAV	122.8	679	32	
19 Jan. 2015	UAV	94.5	1262	39	
13 Feb. 2015	ALS	4.1			CL
8 Mar. 2015	ALS	3.8			PWN
21 Apr. 2015	UAV	76.4	1391	39	year 2
16 Feb. 2016	ALS	4.1			CL
1 Apr. 2016	UAV	112.7	1236	33	year 3

[1] Point density is the spatial mean.
[2] Number of markers and images applies to UAV surveys only.
[3] CL indicates an annual Coastal Lidar survey.

increasingly used to map subaerial coastal morphology (e.g., Mancini et al., 2013; Goncalves and Henriques, 2015) and to monitor its change (e.g., James and Robson, 2012; Casella et al., 2016; Long et al., 2016; Turner et al., 2016). The May13 survey was flown with a fixed-wing Trimble X100 (by a commercial contractor), the remaining surveys were flown with a fixed-wing Easystar I equipped with a 12.1 Mpixel Canon Powershot D10. For each survey, a 3D point cloud was generated from the collected RGB images using a Structure-from-Motion (SfM) and Multiview Stereo (MvS) approach (e.g., James and Robson, 2012; Fonstad et al., 2013; Eltner et al., 2016). We have no detailed knowledge of the SfM-MvS workflow imposed by the contractor for the image processing of the first flight. For the other UAV surveys, about 700 to 1400 aerial photographs were collected (Table 1), and we applied the SfM-MvS workflow contained in AgiSoft Photoscan®Professional Edition. This workflow, described in detail by Javernick et al. (2014) and Brunier et al. (2016), produces a 3D point cloud in a relative coordinate scheme. To allow georeferencing of the point cloud to the RD system, up to 40 circular ground control points (GCPs, Table 1) were positioned throughout the entire study area during each survey. The centres of all GCPs were measured with an RTK-GPS with an horizontal and vertical accuracy of about 0.02 and 0.04 m, respectively, and later on identified in the images within AgiSoft. While the transformation of the AgiSoft to the RD coordinate system is a linear operation, the identification of all GCPs in all corresponding images was also used to non-linearly optimize various camera calibration parameters such as radial and tangential lens distortion coefficients. This is an essential step in improving the positional accuracy of the 3D point cloud (e.g., Javernick et al., 2014; Brunier et al., 2016), as small errors in the distortion coefficients may lead to doming in the z field (e.g., Chandler et al., 2005; Fryer and Mitchell, 1987; James and Robson, 2014). Visual inspectation of the georeferenced and optimized point clouds revealed substantial irregularities in regions composed of wet sand (i.e., the intertidal beach; see also Brunier et al., 2016; Long et al., 2016) and in a narrow strip around the boundary of the point cloud where the number of collected images was rather low. These irregularities were removed manually from the point cloud. The retained points were then processed into a DEM on the same regular 500 × 800 m grid using the exact same methodology as applied to the ALS data points. As can be deduced from Table 1, the density of the UAV-generated point clouds (typically, 50–150 points/m^2) exceeds the ALS point density substantially. The May13 DEM is the first DEM derived after work on all five notches was finalized. Finally, a georeferenced orthophoto of the study site was produced for each UAV survey with a 1 × 1 m (i.e., identical to the DEMs) and a 0.2 × 0.2 m resolution, the latter for improved visualization purposes.

3.2.2. Accuracy

Summary statistics of the *xyz* residuals for the GCPs, as provided by AgiSoft, are shown in Table 2 and include the root-mean-square error (ϵ_{rms}) for the x, y and z coordinates separately and the total ϵ_{rms}. The ϵ_{rms} for x and y were typically 0.015–0.025 m, while those for z were slightly larger at about 0.03 m. The resulting total ϵ_{rms} were typically between 0.04 and 0.05 m. Overall, the *xyz* residuals are about the same as the *xyz* accuracy of the RTK-GPS used to measure the GCP coordinates. Further analysis indicated no spatial dependence of the *xyz* deviations for the individual GCPs. In particular, we did not observe any bowl-shaped (doming) error field; apparently, the camera calibration parameters were sufficiently optimized with the GCPs.

An additional assessment of the z accuracy was performed for the Jan15, Apr15 and Apr16 surveys using points collected with the RTK-GPS. The number of points for Apr16 exceeded that for the other two surveys substantially (Table 3) as the RTK-GPS was mounted on a survey wheel and set to record an observation every second, while the RTK-GPS was operated in stop-and-go point mode during the other two surveys. For each collected RTK-GPS point the z of the closest point from the corresponding georeferenced and optimized point cloud was extracted. For each survey the mean difference (or, bias) b and standard deviation s were computed as error measures, where positive b implies the UAV z to exceed the RTK-GPS z on average. As can be seen in Table 3, b was always positive, but small (< 0.055 m). The s was about 0.07–0.11 m, thus exceeding the ϵ_{rms} computed for the GCPs by a factor of 2–3, but comparable to the ALS accuracy.

It is important to realize that this accuracy assessment is based on GCPs and RTK-GPS points from regions with no vegetation or where the vegetation was less than 1–2 cm in height; in other words, all z were actual ground-surface values. The study site contains, however, various regions where the vegetation was, at least initially, substantially higher. The marram grass on the foredune is typically 0.5 m high, while buckthorn (*Hippophae rhamnoides*) shrubs further landward can reach 1–1.5 m in height. As photogrammetry will produce the elevation of the vegetation top (e.g., Lane et al., 2000; Westaway et al., 2003; Westoby et al., 2012; Javernick et al., 2014), there is thus substantial mismatch between the calculated z and the desired ground-surface value in these vegetated regions. This is explored further in Appendix A, where also a methodology is proposed to minimize the vegetation-induced errors. In the following we refer to all ALS

Table 2
Error statistics for the GCPs[1].

Survey	$\epsilon_{rms}x$ (m)	$\epsilon_{rms}y$ (m)	$\epsilon_{rms}z$ (m)	Total ϵ_{rms} (m)
Apr14	0.020	0.014	0.028	0.038
Oct14	0.023	0.022	0.028	0.043
Jan15	0.018	0.016	0.031	0.039
Apr15	0.022	0.022	0.039	0.049
Apr16	0.025	0.025	0.029	0.045

[1] Error statistics were not provided by the contractor for the May13 survey.

Table 3
Elevation error statistics for the independent RTK-GPS points.

Survey	N[1]	b (m)	ϵ_{rms} (m)
Jan15	147	0.029	0.084
Apr15	262	0.053	0.107
Apr16	3191	0.014	0.067

[1] N is the number of RTK-GPS points.

DEMs and vegetation-corrected UAV DEMs as Digital Terrain Models, DTMs.

3.3. DTM analysis

Geomorphic change in the study area was quantified from the DTMs using transects and sand budget computations. Ten transects were extracted from each DTM (Fig. 6) to illustrate two-dimensional variations in bed elevations of the beach-notch-dune system. For each notch a 'dune-normal' transect was defined, starting at the beach and oriented in the shore-normal direction, over the (initially) deepest part of the notch floor, and extending into a landward dune slack where (with time) most sand was deposited. Also, for each notch a 'dune-parallel' transect was extracted, oriented perpendicularly to the notch floor. The location of all transects was fixed over time.

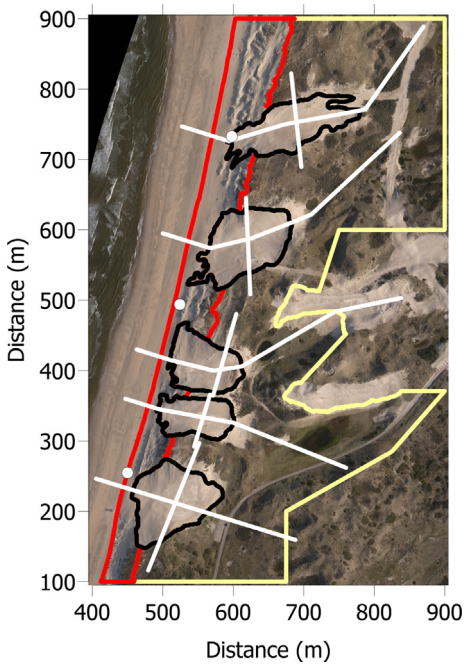

Fig. 6. Outline of the cross-dune and along-dune transects (white lines) to illustrate two-dimensional variations in bed elevations of the beach-notch-dune system and of the three morphological units (*i*: black lines, *ii*: red line; and *iii*: yellow line) used in the sand budget computations. (For interpretation of the references to colour in this figure legend, the reader is referred to the web version of this article.)

For the sand budget computations, the study site was delineated into three discrete geomorphic units: (*i*) the 5 notches, (*ii*) the seaward slope of the foredune between the 2-m and 15-m contours, and (*iii*) the remainder of the foredune and the landward dunes. The initial outline of the notches was determined as the −0.2-m contour from the $\Delta z = z_{Jan13} - z_{Feb12}$ model for N4 and N5 and from $\Delta z = z_{May13} - z_{Feb12}$ for N1, N2 and N3. The value of −0.2 m was chosen because it is approximately $-2s$ in the ALS and UAV data. The second unit was defined between the 2-m and 15-m contours on the seaward face of the foredune because they delimit the region where most wind-blown sand was deposited in the years prior to notch excavation (Fig. 1b). The contours were determined from z_{Feb12}, with the 15-m contour modified to exclude the notches. The southern and northern boundary of this unit were defined by the limits of the study region ($y = 100$ and 900 m, respectively). The third unit extended landward of the 15-m contour and the notches, excluding those parts of the parabolic dunes affected by the vegetation removal. Also, the southeastern part of the study region was not included in this unit (see Fig. 6) because the UAV DTMs did not always include this part of the study site. The ALS DTMs indicated minimal morphological change here (see Section 3.1); its exclusion thus did not bias our sand budget computations. With time the outline of the notches was adjusted to reflect the local retreat of some of the notch walls. This adjustment obviously demanded analogous modifications to the limits of the other two units.

Prior to the sand budget computations random grid cell-size variability (due to observational noise in the ALS and UAV data) from each Δz model (e.g., Passalacqua et al., 2015) was removed using a guided edge-preserving smoothing filter (He et al., 2013). In this way, the undesired small-scale variability was removed effectively but spatially sharp transitions in Δz (e.g., the edges of growing sedimentation lobes) were retained. Because of the large size of the geomorphic units the filtering did not affect the sand budget computations. Its purpose was primarily to enhance the features of interest and, in this way, to create visually more appealing Δz maps.

4. Results

A visual impression of the change in the study area over the 3 years since notch excavation is provided in Fig. 7 using orthophotos taken each year in spring (i.e., at approximately the same moment in the growing season). It is immediately obvious that the notches remained non-vegetated and that the area of bare sand landward of the notches increased markedly with time. For example, the dune slack landward of N3 (Kattendel) was still vegetated in April 2014. One year later all vegetation was covered by sand and the small lake had been filled in. The lateral growth of similar sand surfaces can be seen from the landward end of the other notches. Several buckthorn bushes became completely buried, most notably near N4 and N5 (e.g., Fig. 5d). Also the dense cover of marram grass on the remaining parts of the foredune between the notches changed into active sand surfaces. Observations in the field revealed that marram grass was still present here, but that the density of marram grass had become too low to be seen in the orthophotos. Based on the sand-vegetation maps computed from the orthophotos in Fig. 7, the fraction of sand cover within unit *iii* (i.e., landward of the 15-m contour and the notches) increased from ≈ 33% in May 2013; to 44% in April 2014; to 55% in April 2015; and to 75% in April 2016. The remaining vegetation was located primarily on top of the higher parts of the parabolic dunes and landward of the growing sand surfaces.

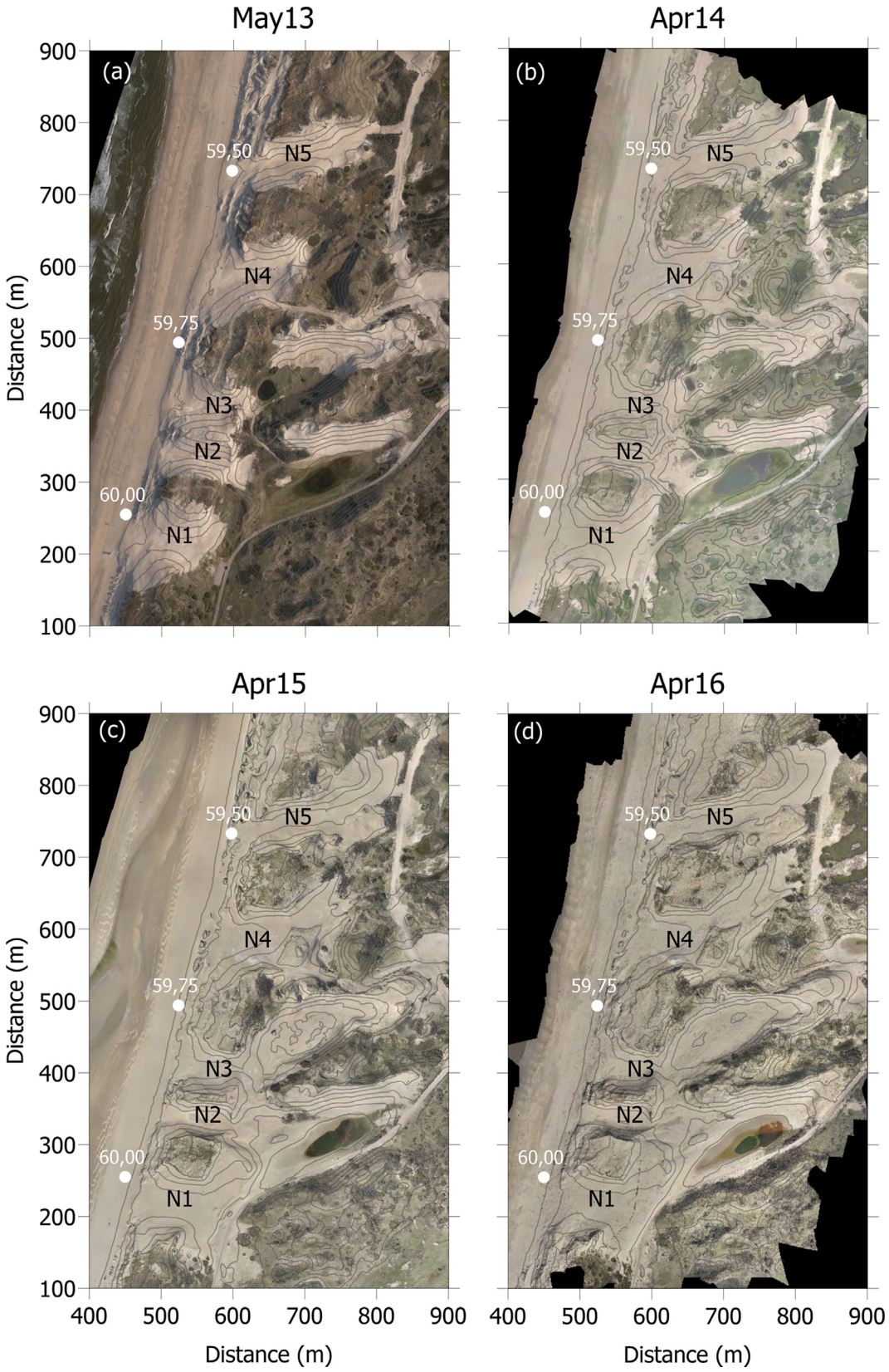

Fig. 7. Orthophotos of the study area in (a) May 2013, (b) April 2014, (c) April 2015 and (d) April 2016. The gray contours in all panels are bed elevation, starting at 3 m MSL and with a 3-m interval.

Depositional lobes formed downwind of the notches (Fig. 8, see also Figs. 5c–d). The lobes at N4 and N5 were clearly the largest. After 3 years they had attained a length of some 125 m and locally, a maximum thickness of more than 8 m (N4) and 4.5 m (N5). Near N2 and N3 the lobe length was then about 55 m, with local maximum thickness of approximately 4.5 m. In more detail, the growth of the N3 lobe coincided with a gentle infilling of the entire dune slack floor (Kattendel) after April 2015. By April 2016 the thickness of this sand blanket varied between 0.3 and 1.3 m along the imposed transect (Fig. 8), which, as was deduced from Fig. 7, was sufficient to bury the pre-existing vegetation of (predominantly) Creeping Willow (*Salex Ripens*). The lobe at N1 did not develop well during the first year, which was caused by human intervention (Section 2). By April 2016 the lobe had extended 40 m in a dune-normal direction and was up to 3 m thick. Its development is, however, hampered by the need to occasionally remove sand from the bicycle track.

Bed elevation change on the notch floors was minimal except in the narrowest notch, N2 (Fig. 8). Here, the central part of the notch floor eroded by almost 1 m/yr, but the seaward and landward ends remained at about 6 and 9 m above MSL. The lateral walls of all notches eroded considerably during the period under study, especially the (northern) wall that is exposed to the dominant southwesterly winds (see also Byrne, 1997). Here, bed elevation dropped locally by over 4 m between May 2013 and April 2016 (Fig. 9). The erosion caused the constructed V-shape to develop into a more U-shape, with a wider (viewed onshore) notch floor and steeper lateral walls. During our (UAV) site visits we observed that, from the second year, the walls developed a distinct composite appearance with a 1-m or more high upper vertical cliff in the root zone of the marram grass overlying a zone inclining near the angle of repose (Fig. 5e). This latter zone was composed of sand that had avalanched or slumped down and extended on to the notch floor. Near the center of the notches, from where the profiles in Fig. 9 were extracted, this mass movement caused the northern wall to recede slightly over the study period (see N1, N2 and N3 in Fig. 9). Based on the computed notch outlines, the largest wall recession (≈ 5 m) took place in the northwestern part of N2, between March 2015 and April 2016. Pedestrian trampling forced a very localized retreat of the northern wall in N1. On the whole, however, the surface enlargement of the notches during the first 3 years after excavation was small, less than 1%. Finally, sand was deposited not only in the sand lobes landward of the notches, but also in a 10–20-m wide zone on top of the foredune extending sideways from all lateral walls (Fig. 9). The deposition depth after 3 years was typically 0.5–1.0 m, with maximum values near 1.5 m (e.g., on top of the northern N1 wall, and the southern N5 wall).

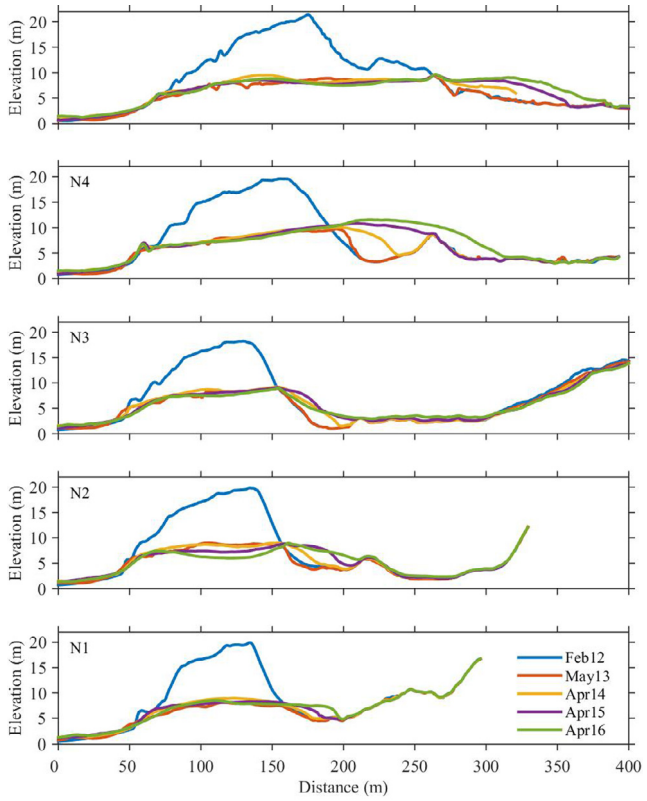

Fig. 8. Elevation z with respect to MSL versus distance (sea to land) along the dune-normal transects shown in Fig. 6. The legend for N1 applies to all panels. Here, Feb12 is the pre-notch topography, while May13 is the topography immediately after work on all notches had completed. Apr14, Apr15 and Apr16 are thus approximately 1, 2 and 3 years after notch excavation, respectively.

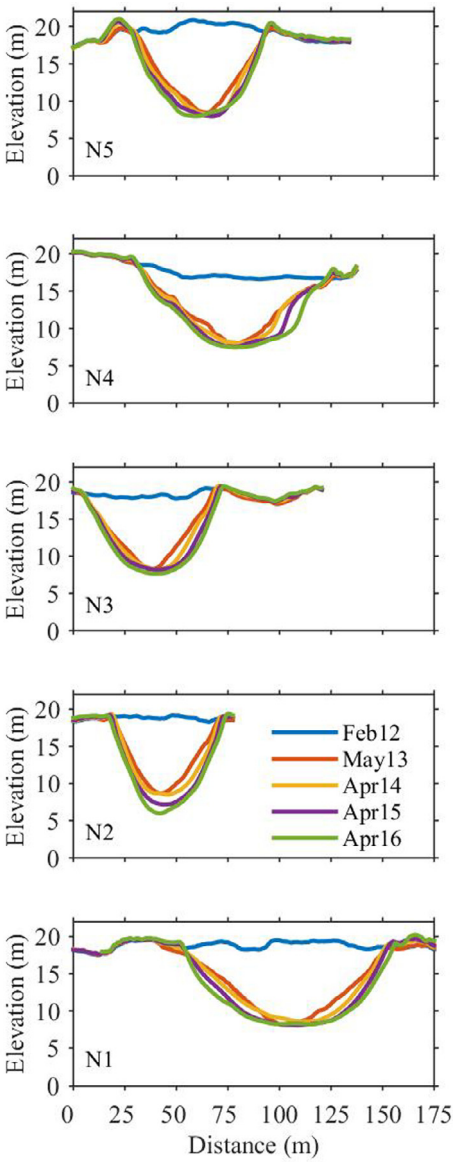

Fig. 9. Elevation z with respect to MSL versus distance along (south to north) the dune-parallel transects shown in Fig. 6. The legend for N2 applies to all panels. Here, Feb12 is the pre-notch topography, while May13 is the topography immediately after work on all notches had completed. Apr14, Apr15 and Apr16 are thus approximately 1, 2 and 3 years after notch excavation, respectively.

The erosion of the lateral walls was initially (April 2014) localized where the notch floor was narrowest (compare Fig. 10b with Fig. 10a), and with time extended spatially to affect almost the entire wall surface by April 2016 (Fig. 10d). The asymmetry in notch erosion is also obvious from Fig. 10b–d, except for N5, where both lateral walls tend to have similar lowering in bed elevation. The location and lateral extension of the depositional lobes at N2–N5 was topographically controlled, as the sand accumulated

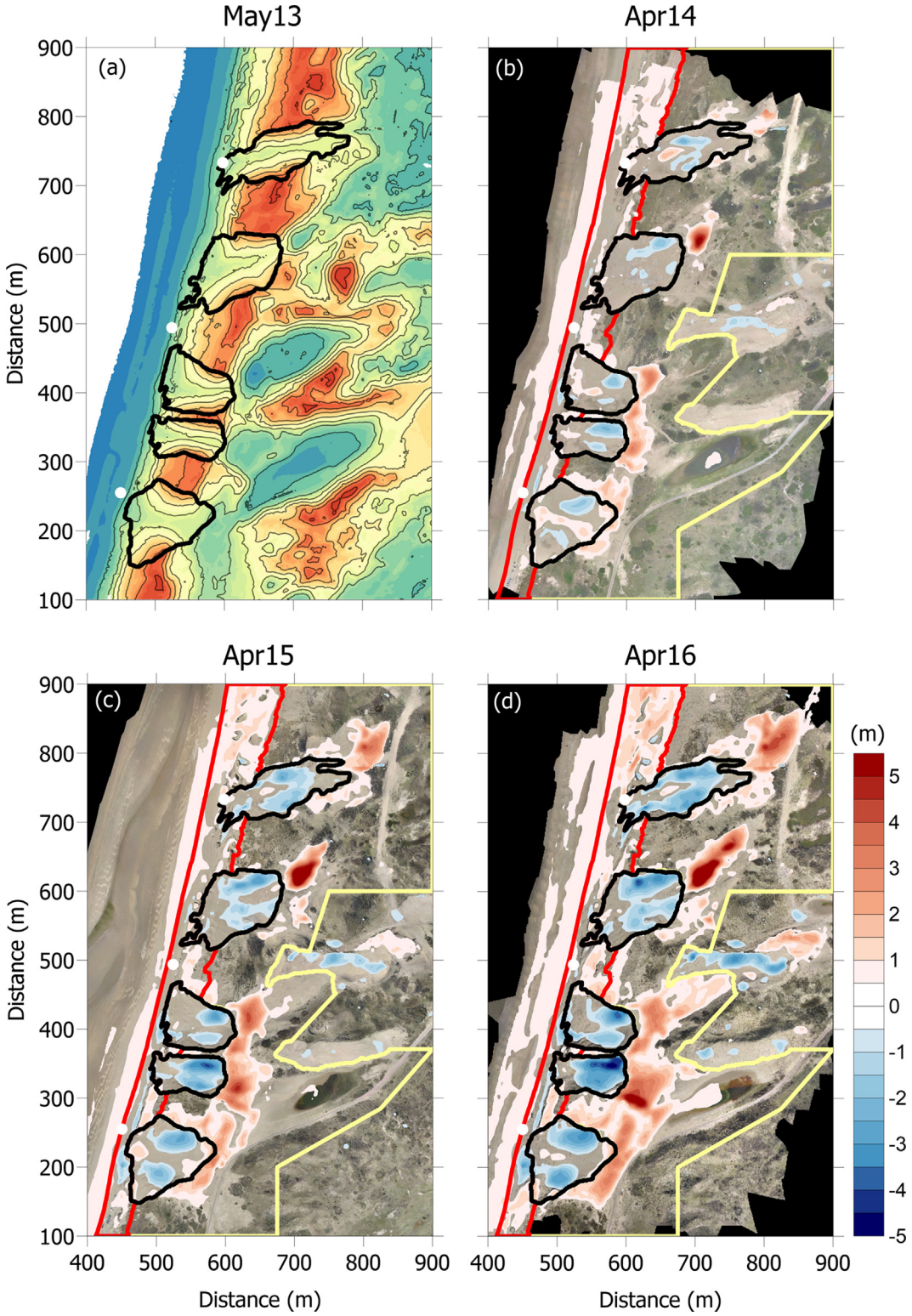

Fig. 10. Bed-elevation change maps with respect to May 2013 for (b) April 2014 ($\Delta z = z_{Apr14} - z_{May13}$), (c) April 2015 ($\Delta z = z_{Apr15} - z_{May13}$), and (d) April 2016 ($\Delta z = z_{Apr16} - z_{May13}$) on top of the corresponding orthophotos. (a) shows the DTM of May 2013 for reference. The color bar next to (d) applies to (b) and (c) as well; note that $\Delta z \pm 0.5$ m is not shown for clarity. The black, red and yellow lines outline the three morphological units used in the sand budget computations. The thin black lines in (a) are bed-elevation contours, starting at 3 m MSL and with a 3-m interval. The color bar for (a) is equal to that of Fig. 4b and is not repeated here for clarity. (For interpretation of the references to colour in this figure legend, the reader is referred to the web version of this article.)

in the dune slacks landward of the foredune, including Peperedel at N2 and Kattendel at N3. The lobe landward of N5 initially had the same orientation as the notch (imposed by the local topography), but as it grew into the broad Houtglop dune slack, its orientation became more north-eastward, that is, aligned with the dominant regional wind direction. In April 2016 the landward end of the lobe at N1 closely followed the bicycle track ($x \approx 600$ m and $y \approx 200$ m in Fig. 10d), induced by the occasional removal of sand that had accumulated on this track. Observations in the field and the elevation change maps further indicate that a substantial part of the sand blown through N1 may have been transported north-eastward to be deposited on the steep south-western slope of Peperedel ($x \approx 600$ m and $y \approx 300$ m in Figs. 10c and d) extending from N2. The narrow alongshore band of negative bed elevation change between the seaward entries of N1 and N2 reflect the erosional impacts (scarping) of storms in December 2013 and October 2014. Further north (N3–N5) scarping was substantially less pronounced or even absent. Here, the seaward side of the foredune (unit *ii*) clearly accreted over the time period considered.

Time series of volumetric change ΔV in the three landscape units since May 2013 are depicted in Fig. 11a. Over the 3-year study period, the notches lost approximately 39,000 m^3, which is equivalent to almost 25% of the volume removed during notch excavation. During the same period, some 87,000 m^3 accumulated landward of the notches, a unit-averaged deposition of some 0.58 m in 3 years. The sum of ΔV_i and ΔV_{iii} (= 48,000 m^3 after 3 years) is the volume of sand that has been blown through the notches and originates from the (intertidal) beach. The total budget change, that is, $\Delta V_i + \Delta V_{ii} + \Delta V_{iii}$, is the total amount of sand blown from the (intertidal) beach into the study area. This volume change, shown in Fig. 11b, increased linearly with time, with the slope of the best-fit line amounting to $\approx 22,750$ m^3/year. If we assume that this sand all originated from the approximately 850-m long beach fronting the study area, the alongshore-averaged input was about 26.5 m^3/m/year. This number is similar to the volume gain of the foredune in the years preceding notch excavation (≈ 27 m^3/m/year, Section 2). Whereas in those years all the wind-blown sand deposited on the seaward side of the foredune, between May 2013 and April 2016 most sand was blown through the notches and deposited inland (unit *iii*). More specifically, in April 2016 the ratio of $\Delta V_i + \Delta V_{iii}$ to ΔV_{ii} was 3.1:1, implying that roughly three times more sand deposited landward of the foredune than on its seaward side. In the years preceding notch construction this ratio was 0. The 3.1:1 ratio at the end of the observational period clearly reflects that the notches have acted as highly effective conduits for aeolian transport into the landward dunes.

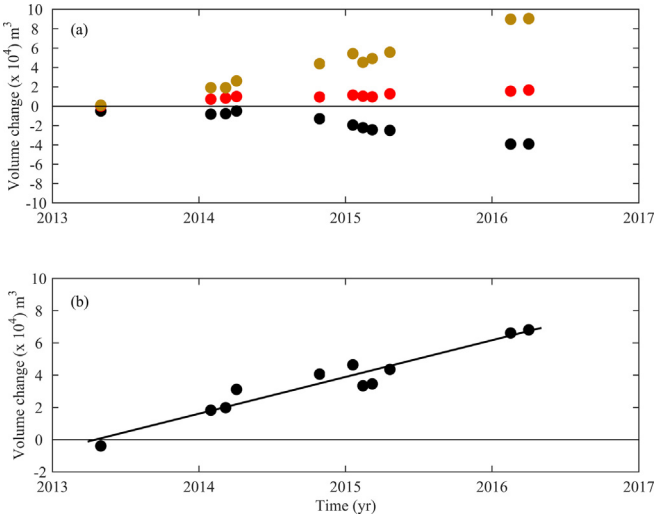

Fig. 11. (a) Time series of volume change ΔV in the three morphological units (*i*: notches, black dots; *ii*: seaward side of foredune, red dots; *iii*: landward of foredune and notches, golden dots) after notch excavation. The values are corrected for the (minor) change in and landward of N4 and N5 between January and May 2013 to fully quantify volumetric change since notch excavation, hence the small negative change in unit *i* (notches; ΔV_i) and positive change in unit *iii* (ΔV_{iii}) in May 2013. (b) displays the estimated volume change ΔV due to aeolian input from the (intertidal) beach. The solid line is best-fit linear line ($r = 0.96$). (For interpretation of the references to colour in this figure legend, the reader is referred to the web version of this article.)

5. Discussion

Since notch excavation aeolian activity (erosion, transport and deposition) in and immediately landward of the foredune has increased, new aeolian landforms have developed (e.g., composite notch walls and depositional lobes), the area of active sand has enlarged, and the sand budget landward of the foredune has become positive. This is quite different from outcomes reported by Riksen et al. (2016), who found minimal sand supply landward of narrow (≈ 20 m), isolated notches; but consistent with the preliminary findings of the functioning of multiple, closely spaced notches along the Welsh coast (Pye and Blott, 2016), especially those fronting wide and high beaches. Although the coastal dunes in our study area are now among the most dynamic along the Dutch coast and, accordingly, the area of the Natura2000 habitat White Dunes (H2120) has extended substantially, it remains to be established whether the increased landscape diversity leads to floral and faunal pioneer species and hence to an overall higher species diversity. Currently, the lobes advance downwind into the vegetation (Fig. 7) and the resulting sand burial presumably causes biodiversity to decline. The results of vegetation mapping (Arens et al., 2016) and entomological research (De Rond, 2016) illustrate that aeolian processes on the lobes are currently too dynamic for floral and faunal species to establish. We expect that, as the lobes evolve further, aeolian dynamics at their lateral edges will locally diminish, opening up conditions that favour early-stage or mid-stage successional plant species and, therefore, result in an increase in biodiversity to a level that exceeds pre-notch species diversity substantially. This may take tens of years. Nordstrom et al. (2007) reported such trends in biodiversity landward of a small gap in a foredune near Ocean City, New Jersey, USA. The number of species was observed to decline in regions buried by sand blown through the gap; in contrast, the stabilization of bare sand patches by American marram grass (*Ammophila breviligulata*) initiated the establishment of species that are less adapted to stressful environments, resulting in an overall higher species richness in the dune system. The notches in our study area may also be beneficial to the biodiversity in the Natura2000 habitat Grey Dunes (H2130). Multi-year measurements with sand traps show that some sand is blown hundreds of meters inland of the notches (Arens et al., 2016). This is not the case in regions where notches are absent. The deposition of this calcareous sand is likely to counteract present-day soil acidification by atmospheric N-deposition and thus to result in conditions that are more favourable to the endemic dune flora in the Grey Dunes area (e.g., Aggenbach et al., 2016).

Observations of the dynamics of trough blowouts, the natural equivalents of excavated foredune notches, may indicate whether the notches remain effective conduits for aeolian transport into the more landward dunes. Based on observations at Island Beach State Park, New Jersey, Gares and Nordstrom (1995) presented a conceptual model that comprises distinct stages of blowout opening, growth and closing because of feedbacks between the

dune morphology, wind flow and vegetation. The foredune notches in our study area are developing similarly as trough blowouts in their growth stage. The steepening and retreat of the lateral walls because of the avalanching and slumping of material on to the notch floor (Figs. 5e and 9), the asymmetry in this erosion because of the onshore shore-oblique wind climate (Figs. 9 and 10) and rim deposition (Fig. 10) have all been reported for growing trough blowouts by, for example, Carter et al. (1990), Gares (1992)), Hesp and Hyde (1996) and Byrne (1997). In the Gares and Nordstrom (1995) model the trough widening initiates the closing stage of the blowout, because the resulting reduced acceleration of the wind flow opens up opportunities for vegetation regrowth. This stabilizes the blowout and enforces its (partial) infilling. Vegetation regrowth may initially be most marked at the outline of the depositional lobes, which may cause them to evolve into parabolic dunes (e.g., Hesp and Walker, 2011). Vegetation can also develop in the throat of the blowout (e.g., Hesp, 2002; Battiau-Queney, 2014), resulting in the growth of incipient foredunes, which may block the influx of beach sand and hence also lead to blowout closure. We note that the Gares and Nordstrom (1995) model was based on observations of blowouts in different stages of their evolution rather than of a single blowout successively going through all stages. We do not know whether the model is also applicable to closely spaced excavated notches that are in the same stage and may, if the widening continues, start to affect each other's development. The widening of the individual notches may cause them to eventually merge, producing one or more large deflation basins. Such behaviour has been observed in a dune restoration project on the Dutch barrier island Terschelling, although the development of the deflation basin was likely stimulated by vegetation removal from the foredune between the notches (Arens et al., 2007, 2013). Follow-up monitoring is adamant to answer the question how the foredune notches will develop further and whether they are, as hoped, self-maintaining measures for dune restoration.

6. Conclusions

Based on repeat high-resolution (1×1 m) topographic survey data collected with airborne Lidar and UAV photogrammetry, we have shown that the five foredune notches in the 20-m high established foredune of the Dutch National Park Zuid-Kennemerland have strongly increased dune dynamics during the first three years since excavation (2013–2016). These dynamics comprise (1) an increase in aeolian erosion, transport and deposition, (2) the development of new aeolian landforms, (3) an increase in the area of bare sand, and (4) a positive sand budget landward of the foredune. Erosion was largely restricted to the lateral notch walls, which with time developed an $\approx$ 1-m high upper vertical cliff in the root zone of the marram grass overlying a more gently sloping zone comprising material that had avalanched or slumped on to the notch floor. Landward of the notches, up to 150-m long and 8-m thick depositional lobes formed that locally buried buckthorn shrubs. The positive sand budget of the total study area after notch excavation ($\approx 22,750$ m^3/year) was about equal to the pre-notch situation (2006–2012). While in those years all sand accumulated on the seaward side of the foredune, 75% of the sand has deposited landward of the foredune since notch excavation. This implies that the notches have been acting as highly effective conduits for aeolian transport into the landward dunes. Future work needs to elucidate whether the increased landscape diversity will, as intended, result in an overall higher floral and faunal species diversity, and for how long the notches will remain effective measures for dune restoration.

Acknowledgements

We thank Marcel van Maarseveen, Henk Markies, Hans Windmüller and Maarten Zeylmans van Emmichoven for their excellent support in collecting and/or providing the topographic data, Christian Schwarz for discussions on the future evolution of the notches, and two referees for their review and extensive comments on the text. The Noordwest Natuurkern project is part of the Dutch Dune Revival project, financed by the European LIFE+ Regulation and the province of North-Holland (LIFE09 NAT/NL/000418). The research presented here was supported by the Dutch Technology Foundation STW (Vici project 13709), which is part of the Netherlands Organisation for Scientific Research (NWO), and which is partly funded by the Ministry of Economic Affairs.

Appendix A. Vegetation removal from UAV-derived DEMs

In vegetated regions photogrammetry produces the elevation of the vegetation top rather than the desired ground-surface values. An example hereof is shown in Fig. A1a–b. The difference in elevation Δz between the UAV-Apr14 and ALS-Mar14 DEMs, $\Delta z = z_{\mathrm{Apr14}} - z_{\mathrm{Mar14}}$, shows isolated dark-red ($\Delta z > 1$ m) patches (Fig. A1b), which correspond to buckthorn shrubs (the dark green patches in the orthophoto, Fig. A1a). Also, the vegetated foredunes show spatially extensive Δz of 0.2–0.5 m (Fig. A1b), which relates to marram grass. The vegetation-induced mismatch needs to be minimized to jointly use ALS and UAV based DEMs in the analysis of the geomorphological evolution of the entire study area.

To achieve this, each 1×1-m orthophoto was converted into a binary sand-vegetation image using the ExGminExR vegetation index (Meyer and Neto, 2008) and the Otsu (Otsu, 1979) threshold selection method. The ExGminExR index is the difference between Excess Green ExG (Woebbecke et al., 1995) and Excess Red ExR (Meyer et al., 1998), which are defined as $\mathrm{ExG} = 2\mathrm{G} - \mathrm{R} - \mathrm{B}$ and $\mathrm{ExR} = 1.4\mathrm{R} - \mathrm{B}$. Here, R, G and B are the 8-bit brightness intensities of the Red, Green and Blue channels, respectively. The greenness of the vegetation and the redness of the sand cause vegetation and sand to have high ExG and ExR, respectively, as well as low ExR and ExG. By taking the difference between ExG and ExR, ExGminExR, the difference between vegetation and sand is thus further increased. The threshold selection method of Otsu (Otsu, 1979) was then applied to segment an ExGminExR map into a binary sand (0) and vegetation (1) map, see Fig. A1c for the result based on the orthophoto in Fig. A1a. Finally, each z of a vegetation pixel was replaced by the z at the same (x, y) coordinate of the nearest (in time) ALS DEM. This assumes that ground-surface values beneath vegetation did not change with time. The corrected $\Delta z = z_{\mathrm{Apr14}} - z_{\mathrm{Mar14}}$ map is shown in Fig. A1d. It no longer contains the positive Δz on the vegetated parts of the foredune and at the buckthorn shrubs, but the non-zero Δz on the beach and near the notches are retained. These most likely resulted from the growth and landward migration of an intertidal sandbar and the growth of depositional lobes, respectively.

In contrast to Meyer and Neto (2008), we did not normalize the RGB channels prior to the computation of ExGminExR to correct for different light conditions, because it was not obvious how their normalization method should be implemented here. Meyer and Neto (2008) found $\mathrm{ExGminExR} = 0$ as an appropriate threshold value in their normalized agricultural plant-soil image data set and, accordingly, they abandoned the Otsu (1979) step. In our case, the threshold value was substantially different between surveys, varying between -76 and -61. It would seem that the different

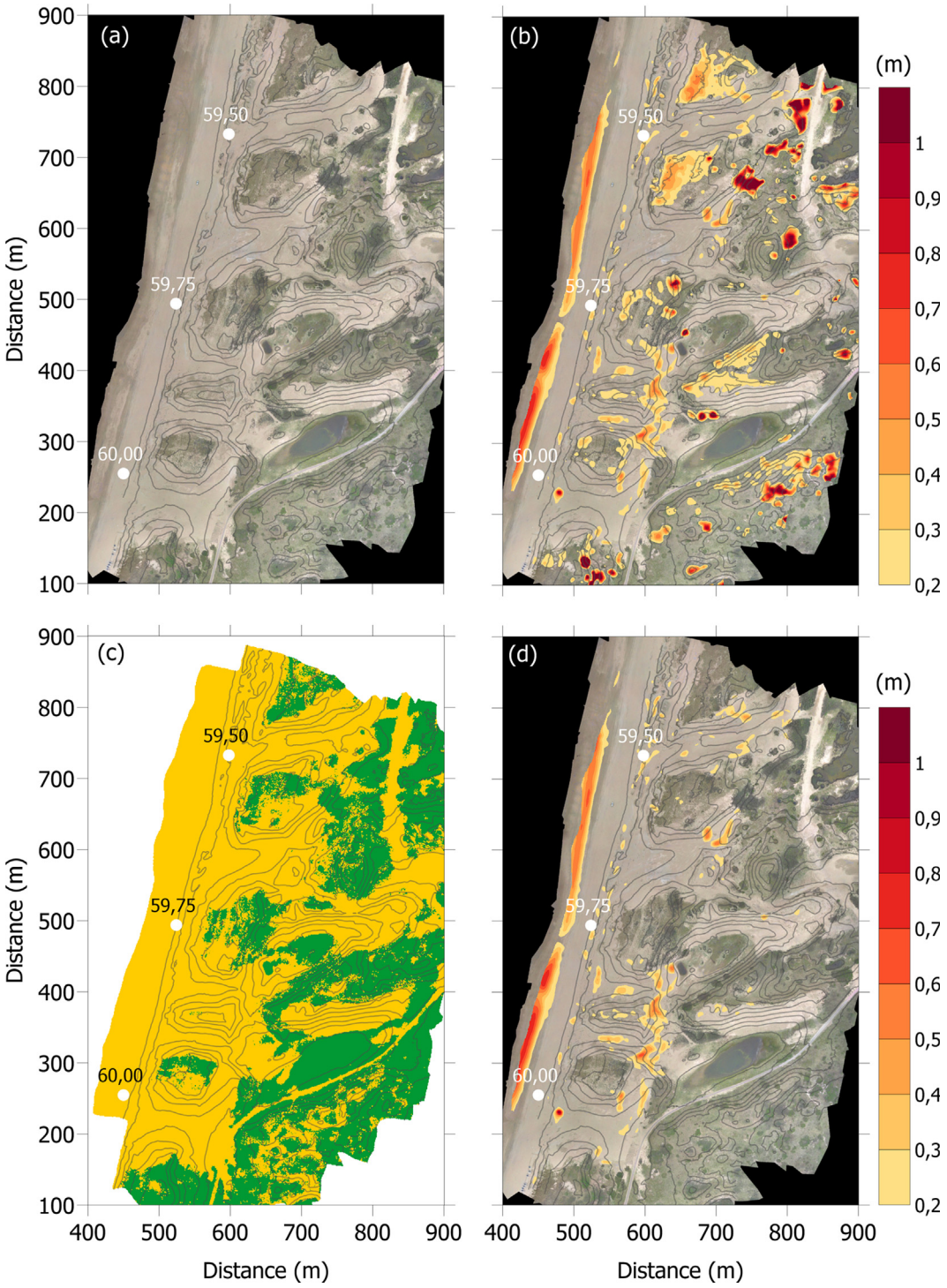

Fig. A1. Illustration of the vegetation-removal algorithm using the (a) Apr14 orthophoto as example. In (b) the positive differences in elevation Δz between the UAV-Apr14 and ALS-Mar14 DEMs are shown with the yellow-brown colours. Panel (c) illustrates the binary sand (yellow)–vegetation (green) map computed from the orthophoto in (a). Panel (d) is the same as (b), but now based on the UAV-Apr14 DTM. The gray contours in all panels are bed elevation, starting at 3 m MSL and with a 3-m interval. (For interpretation of the references to colour in this figure legend, the reader is referred to the web version of this article.)

light conditions between UAV surveys were compensated for in the threshold value to delineate vegetation from sand. The ExGminExR method fails on shaded sand regions, which are incorrectly classified as vegetation with the threshold selection method. This situation happened on north-facing slopes for Oct14 and Jan15. The affected regions were identified manually and corrected to sand (0). The study area also contains non-sand and non-vegetation elements, such as the pavement of a bicycle track and water (the shallow lakes in the dune slacks of Peperedel and Houtglop). These additional two features were classified as sand and vegetation with the present methodology, respectively. This did not noticeably affect the sand budget computations presented in Section 4, as here UAV- and Lidar-based elevations were essentially identical.

References

Aggenbach, C.J.S., Arens, S.M., Kooijman, A., Lammerts, E.J., 2016. Beheersadvies activering eolische dynamiek op de Waddeneilanden als PAS-maatregel voor habitattype H2130 Grijze duinen, in Dutch.

Arens, B., Geelen, L., 2001. Geomorfologie en regeneratie van duinvalleien. Het Landschap 18, 133–146. in Dutch.

Arens, B., Geelen, L., Van der Hagen, H., Slings, R., 2012. Is zandaanvoer door de zeereep de sleutel tot succes? Het Landschap 29, 131–139. in Dutch.

Arens, B., Neijmeijer, T., Van Tongeren, O., 2016. Noordwestkern: effecten van ingrepen op dynamiek - resultaten monitoring 2013–2015. Tech. Rep. 2015.09, Arens BSDO, in Dutch.

Arens, S.M., 1999. Evaluatie dynamisch zeereepbeheer - vergelijking situatie 1988 en 1998. Tech. Rep. RAP99.01, Ministerie van Verkeer en Waterstaat, Rijkswaterstaat, Dienst Weg- en Waterbouwkunde (RWS, DWW), in Dutch.

Arens, S.M., Geelen, L.H.W.T., 2006. Dune landscape rejuvenation by intended destabilisation in the Amsterdam Water Supply Dunes. J. Coastal Res. 225, 1094–1107.

Arens, S.M., Löffler, M.A.M., Nuijen, E.M., 2007. Evaluatie dynamisch kustbeheer Friese Waddeneilanden. Tech. Rep. Arens BSDO RAP2006.04, Arens BSDO, in Dutch.

Arens, S.M., Mulder, J.P.M., Slings, Q.L., Geelen, L.H.W.T., Damsma, P., 2013. Dynamic dune management, integrating objectives of nature development and coastal safety: examples from the Netherlands. Geomorphology 199, 205–213.

Arens, S.M., Slings, Q., De Vries, C.N., 2004. Mobility of a remobilised parabolic dune in Kennemerland, The Netherlands. Geomorphology 59, 175–188.

Arens, S.M., Wiersma, J., 1994. The Dutch foredunes: inventory and classification. J. Coastal Res. 10, 189–202.

Battiau-Queney, Y., 2014. The dunes of Merlimont (north of France): a natural museum of aeolian landforms. Coastal Dunes Management Strategies and Practices: Perspectives and Case Studies, vol. 33, pp. 51–65.

Bochev-van der Burgh, L.M., Wijnberg, K.M., Hulscher, S.J.M.H., 2011. Decadal-scale morphologic variability of managed coastal dunes. Coastal Eng. 58, 927–936.

Brunier, G., Fleury, J., Anthony, E.J., Gardel, A., Dussouillez, P., 2016. Close-range airborne Structure-from-Motion photogrammetry for high-resolution beach morphometric ssurvey: examples from an embayed rotating beach. Geomorphology 261, 76–88.

Byrne, M.L., 1997. Seasonal sand transport through a trough blowout at Pinery Provincial Park, Ontario. Can. J. Earth Sci. 34, 1460–1466.

Carter, R.W.G., Hesp, P.A., Nordstrom, K.F., 1990. Erosional landforms in coastal dunes. Ch. 11, pp. 217–250.

Casella, E., Rovere, A., Pedroncini, A., Stark, C.P., Casella, M., Ferrari, M., Firpo, M., 2016. Drones as tools for monitoring beach topography changes in the Ligurian Sea (NW Mediterranean). Geo-Marine Lett. 36, 151–163.

Chandler, J.M., Fryer, J.G., Jack, A., 2005. Metric capabilities of low-cost digital cameras for close range surface measurement. Photogramm. Rec. 20, 12–26.

Darke, I.B., Walker, I.J., Hesp, P.A., 2016. Beach-dune sediment budgets and dune morphodynamics following coastal dune restoration, Wickaninnish Dunes, Canada. Earth Surface Processes Landforms 41, 1370–1385.

De Rond, J., 2016. De invloed van verstuivingsdynamiek op de insectenfauna van zeeduinen, in Dutch.

De Ruig, J.H.M., Hillen, R., 1997. Developments in Dutch coastline management: conclusions from the second governmental coastal report. J. Coastal Conserv. 3, 203–210.

De Winter, R.C., Gongriep, F., Ruessink, B.G., 2015. Observations and modeling of alongshore variability in dune erosion at Egmond aan Zee, the Netherlands. Coastal Eng. 99, 167–175.

D'Errico, J., 2004. Inpaintnans. Matlab Central File Exchange, release: 2. URL http://www.mathworks.com/matlabcentral/fileexchange/4551.

Elliott, M., Burdon, D., Hemingway, K.L., Apitz, S.E., 2007. Estuarine, coastal and marine ecosystem restoration: Confusing management and science - A revision of concepts. Estuarine Coastal Shelf Sci. 74, 349–366.

Eltner, A., Kaiser, A., Castillo, C., Rock, G., Neugirg, F., Abellan, A., 2016. Image-based surface reconstruction in geomorphometry – merits, limits and developments. Earth Surf. Dyn. 4, 359–389.

Everard, M., Jones, L., Watts, B., 2010. Have we neglected the societal importance of sand dunes? An ecosystem services perspective. Aquat. Conserv.: Marine Freshwater Ecosyst. 20, 476–487.

Feagin, R.A., Figlus, J., Zinnert, J.C., Sigren, J., Martinez, M.L., Silva, R., Smith, W.K., Cox, D., Young, D.R., Carter, G., 2015. Growing with the flow or against the grain? The promise of vegetation for protecting beaches, dunes, and barrier islands from erosion. Front. Ecol. Environ. 13, 203–210.

Fonstad, M.A., Dietrich, J.T., Courville, B.C., Jensen, J.L., Carbonneau, P.E., 2013. Topographic structure from motion: a new development in photogrammetric measurement. Earth Surf. Processes Landforms 38, 421–430.

Fryer, J.G., Mitchell, H.L., 1987. Radial distortion and close-range stereophotogrammetry. Aust. J. Geod. Photogramm. Surv. 46, 123–138.

Gares, P.A., 1992. Topographic changes associated with coastal dune blowouts at Island Beach State Park, New Jersey. Earth Surf. Processes Landforms 17, 589–604.

Gares, P.A., Nordstrom, K.F., 1995. A cyclic model of foredune blowout evolution for a leeward coast: Island Beach, New Jersey. Ann. Assoc. Am. Geogr. 85 (1), 1–20.

Goncalves, J.A., Henriques, R., 2015. UAV photogrammetry for topographic monitoring of coastal areas. ISPRS J. Phologrammetry Remote Sensing 104, 101–111.

Grootjans, A., Geelen, H.W.T., Jansen, A.J.M., Lammerts, E.J., 2002. Restoration of coastal dune slacks in the Netherlands. Hydrobiologia 478, 181–203.

He, K., Sun, J., Tang, X., 2013. Guided image filtering. IEEE Trans. Patt. Anal. Mach. Intell. 35 (6), 1397–1409.

Hesp, P.A., 2002. Foredunes and blowouts: initiation, geomorphology and dynamics. Geomorphology 48, 245–268.

Hesp, P.A., Hyde, R., 1996. Flow dynamics and geomorphology of a trough blowout. Sedimentology 43, 505–525.

Hesp, P.A., Ruz, M.H., Hequette, A., Marin, D., Da Silva, G.M., 2016. Geomorphology and dynamics of a traveling cuspate foreland, Authie estuary, France. Geomorphology 254, 104–120.

Hesp, P.A., Walker, I.J., 2011. Coastal Dunes, vol. 11. Academic Press, pp. 109–133.

Hilton, M.J., 2006. The loss of New Zealand's active dunes and the spread of marram grass (Ammophila arenaria). In: New Zealand Geographer 62, 105–120.

Jackson, N.L., Nordstrom, K.F., 2011. Aeolian sediment transport and landforms in managed coastal systems: a review. Aeolian Res. 3, 181–196.

Jackson, N.L., Nordstrom, K.F., Faegin, R.A., Smith, W.K., 2013. Coastal geomorphology and restoration. Geomorphology 199, 1–17.

James, M.R., Robson, S., 2012. Straightforward reconstruction of 3D ssurface and topography with a camera: accuracy and geoscience application. J. Geophyis. Res. – Earth Surf. 117 (F03017).

James, M.R., Robson, S., 2014. Migrating systematic error in topographic models derived from UAV and ground-based image networks. Earth Surf. Processes Landforms 39, 1413–1420.

Javernick, L., Brasington, J., Caruso, B., 2014. Modeling the topography of shallow braided rivers using Structure-from-Motion photogrammetry. Geomorphology 213, 166–182.

Jungerius, P.D., Koehler, H., Kooijman, A.M., Mücher, H.J., Graefe, U., 1995. Response of vegetation and soil ecosystem to moving and sod removal in the coastal dunes 'Zwanewater', the Netherlands. J. Coastal Conserv. 1, 3–16.

Klijn, J.A., 1981. Nederlandse kustduinen - geomorfologie en bodems. Ph.D. thesis, Landbouwhogeschool, Wageningen, ISBN 90 220 0768 5.

Konlechner, T.M., Ryu, W., Hilton, M.J., Sherman, D.J., 2015. Evolution of foredune texture following dynamic restoration, Doughboy Bay, Stewart Island, New Zealand. Aeolian Res. 19, 208–214.

Kooijman, A.M., 2004. Environmental problems and restoration measures in coastal dunes in The Netherlands. Springer. Ch. 15.

Koshiek, L.H.M., 1984. De korrelgrootte karakteristiek van de zeereep (stuifdijk) langs de Nederlandse kust. Tech. Rep. WWKZ-84G-282, Rijkswaterstaat – Directie Waterhuishouding en Waterbeweging – District Kust en Zee, (in Dutch).

Kuipers, M., 2014. The daring Dutch: restoring the dynamic dunes. In: Favennac, J., Battiau-Queney, Y. (Eds.), Coastal dunes management strategies and practices: perspectives and case studies. vol. 33 of Dynamiques environnementales. pp. 132–138.

Kuipers, M., Arens, B., Ruessink, G., 2016. Grootschalig herstel van stuivende duinen. De Levende Natuur 117 (3), 89–93 (in Dutch).

Lammerts, E.J., Nijssen, M., Grootjans, A., Kooijman, A., Oost, A., 2009. Het belang van ruimte- en tijdschalen voor ecologisch herstel van het kustlandschap. De Levende Natuur 110, 158–163. in Dutch.

Lane, S.N., James, T.D., Crowell, M.D., 2000. Application of digital photogrammetry to complex topography for geomorphological research. Photogrammetric Record 16, 793–821.

Lithgow, D., Martínez, M.L., Gallego-Fernández, J.B., Hesp, P.A., Flores, P., Gachuz, S., Rodríguez-Revelo, N., Jiménez-Orocio, O., Mendoza-González, Álvarez-Molina, L.L., 2013. Linking restoration ecology with coastal dune restoration. Geomorphology 199, 214–224.

Long, N., Millescamps, B., Guillot, B., Pouget, F., Bertin, X., 2016. Monitoring the topography of a dynamic tidal inlet using UAV imagery. Remote Sensing 8.

Luijendijk, A., De Vroeg, H., Swinkels, C., Walstra, D.J., 2011. Coastal response on multiple scales: a pilot study on the IJmuiden port. In: Coastal Sediments. pp. 602–615.

Mancini, F., Dubbini, M., Gattelli, M., Stecchi, F., Fabbri, S., Gabbianelli, G., 2013. Using Unmanned Aerial Vehicles (UAV) for high-resolution reconstruction of topography: the Structure from Motion approach on coastal environments. Remote Sensing 5, 6880–6898.

Martínez, M.L., Gallego-Fernández, J.B., Hesp, P.A., 2013. Coastal Dunes: Human Impact and Need for Restoration. Springer. Ch. 1, pp. 1–14.

Meerkerk, A.L., Arens, S.M., Van Lammeren, R.J.A., Stuiver, H.J., 2007. Sand transport dynamics after a foredune breach: a case study from Schoorl, The Netherlands. Geomorphology 86, 52–60.

Meyer, G.E., Hindman, T., Laksmi, K., 1998. Machine vision detection parameters for plant species identification. In: Meyer, G.E. (Ed.), Precision agriculture and biological quality. pp. 327–334.

Meyer, G.E., Neto, J.C., 2008. Verification of color vegetation indices for automated crop imaging applications. Comput. Electron. Agric. 63, 282–293.

Nordstrom, K.F., Arens, S.M., 1998. The role of human actions in evolution and management of foredunes in The Netherlands and New Jersey, USA. J. Coastal Conserv. 4, 169–180.

Nordstrom, K.F., Hartman, J.M., Freestone, A.L., Wong, M., Jackson, N.L., 2007. Changes in topography and vegetation near gaps in a protective foredune. Ocean Coastal Manage. 50, 945–959.

Nordstrom, K.F., Lotstein, E.L., 1989. Perspectives on resource use of dynamic coastal dunes. Geograph. Rev. 79, 1–12.

Otsu, N., 1979. A threshold selection method from gray-level histograms. IEEE Trans. Syst. Man Cybern, 62–66. SMC-9.

Passalacqua, P., Belmont, P., Staley, D.M., Simley, J.D., Arrowsmith, J.R., Bode, C.A., Crosby, C., DeLong, S.B., Glenn, N.F., Kelly, S.A., Lague, D., Sangireddy, H., Schaffrath, K., Tarboton, D.G., Wasklewicz, T., Wheaton, J.M., 2015. Analyzing high resolution topography for advancing the undunderstand of mass and energy transfer through landscapes: a review. Earth-Science Rev. 148, 174–193.

Petersen, P.S., Hilton, M.J., Wakes, S.J., 2011. Evidence of aeolian sediment transport across an Ammophila arenaria-dominated foredune, Mason Bay, Stewart Island. New Zealand Geographer 67, 174–189.

Provoost, S., Laurence, M., Jones, M., Edmondson, S.E., 2011. Changes in landscape and vegetation of coastal dunes in Northwest Europe: a review. J. Coastal Conserv. 15, 207–226.

Pye, K., Blott, S.J., 2016. Dune rejuvenation trials: overview report. Report to Natural Resources Wales. Tech. Rep. KPAL Report 19099, Kenneth Pye Associates Ltd.

Pye, K., Blott, S.J., Howe, M.A., 2014. Coastal dune stabilization in Wales and requirements for rejuvenation. J. Coastal Conserv. 18, 27–54.

Riksen, M.J.P.M., Goossens, D., Huiskes, H.P.J., Krol, J., Slim, P.A., 2016. Constructing notches in foredunes: effect on sediment dynamics in the dune hinterland. Geomorphology 253, 340–352.

Schupp, C.A., WInn, N.T., Pearl, T.L., Kumer, J.P., Carruthers, T.J.B., 2013. Restoration of overwash processes creates piping clover (Charadrius melodus) habitat on a barrier island (Assateague Island, Maryland). Estuarine, Coastal Shelf Sci. 116, 11–20.

Sigrin, J.M., Figlus, J., Armitage, A.R., 2014. Coastal sand dunes and dune vegetation: restoration, erosion, and storm protection. Shore Beach 82, 5–12.

Turner, I.L., Harley, M.D., Drummond, C.D., 2016. UAVs for coastal surveying. Coastal Eng. 114, 19–24.

Van Boxel, J.H., Jungerius, P.D., Kieffer, N., Hampele, N., 1997. Ecological effects of reactivation of artificially stabilized blowouts in coastal dunes. J. Coastal Conserv. 3, 57–62.

Van der Putten, W.H., Peters, B.A.M., 1995. Possibilities for management of coastal foredunes with deteriorated stands of Ammophila arenaria (marram grass). J. Coastal Conserv. 1, 29–39.

Van Til, M., Ketner, P., Provoost, S., 2002. Duinstruwelen in opmars. De Levende Natuur 103, 74–77. in Dutch.

Veer, M.A.C., Kooijman, A.M., 1997. Effects of grass-encroachment on vegetation and soil in Dutch dry dune grasslands. Plant Soil 192, 119–128.

Walker, I.J., Eamer, J.B.R., Darke, I.B., 2013. Assessing significant geomorphic changes and effectiveness of dynamic restoration in a coastal dune ecosystem. Geomorphology 199, 192–204.

Westaway, R.M., Lane, S.N., Hicks, D.M., 2003. Remote survey of large-scale braided, gravel-bed rivers using digital photogrammetry and image analysis. Int. J. Remote Sensing 4, 795–815.

Westoby, M.J., Brasington, J., Glasser, N.F., Hambrey, M.J., Reynolds, J.M., 2012. Structure-from-Motion photogrammetry: a low-cost, effective tool for geoscience applications. Geomorphology 179, 300–314.

Woebbecke, D.M., Meyer, G.E., Von Bargen, K., Mortesen, D.A., 1995. Color indices for weed identification under various soil, residue, and lighting conditions. Trans. ASAE 38, 259–269.

Woolard, J.W., Colby, J.D., 2002. Spatial characterization, resolution, and volumetric change of coastal dunes using airborne LIDAR: Cape Hatteras, North Carolina. Geomorphology 48, 269–287.